

## A MICROMACHINED KELVIN PROBE FOR SURFACE POTENTIAL MEASUREMENTS IN MICROFLUIDIC CHANNELS AND SOLID-STATE APPLICATIONS

L.L. Chu<sup>1,2</sup>, K. Takahata<sup>1</sup>, P. Selvaganapathy<sup>1</sup>, J.L. Shohet<sup>2</sup>, and Y.B. Gianchandani<sup>1,2\*</sup>,

<sup>1</sup>EECS Department, University of Michigan, Ann Arbor, USA

<sup>2</sup>ECE Department, University of Wisconsin, Madison, USA

### ABSTRACT

This paper reports on a micromachined Kelvin probe structure with integrated scanning tip and dither actuation mechanism. It is fabricated by a modified micro electro-discharge machining process which allows electrical isolation within the micromachined structure using epoxy plugs. The device is used to measure changes in the external surface potential of a parylene microfluidic channel as a function of varying pH of liquid inside the channel. A contact potential difference of  $\approx 6$  V is measured for a change in pH from 4 to 8 within the channel. The device is also used to map embedded charge in a thin SiO<sub>2</sub> layer on a Si substrate, showing it to be suitable for monitoring microelectronics manufacturing processes.

### 1. INTRODUCTION

Kelvin probes provide non-contact measurement of variations in surface potential, which has two components: work function, and potential due to trapped charge [And52, Sur70, Nab97]. Trapped charge is monitored in semiconductor IC-fabrication because it has been correlated to the degradation of electronic device parameters [Hof97]. Since the Kelvin probe method is a non-contact and non-destructive diagnostic, it can be used to monitor processes that are known to charge wafers, such as plasma etch and deposition, ion implantation, and certain cleaning and wafer drying operations. Conventional plasma damage characterization approaches [Fri97, Cis98, Fan92], are based on electrical or surface analytical techniques, which cannot measure local charge distributions on patterned wafers. The ability to measure local charge distributed across patterns on production wafers can be a critical asset in predicting yield and longevity of devices.

Another potential application for scanning Kelvin probes is the mapping of surface charge in a bio-fluidic channel or tube [Bai98]. Charge distribution on the wall, acquired during manufacturing or in routine operation, can impact the function and behavior of the fluid in the channel. For example, it has been linked to cell adhesion and clotting of red blood cells on artificial surfaces [Mur73]. A Kelvin probe can be used to map the charge embedded in the wall by scanning the outside of the fluidic channel using the electrolyte in the channel as an electrode. Further, as will be shown in this paper, a single point measurement can also be used to provide an indication of the local pH of the fluid.

Relative surface charge density has been measured using atomic force microscopy (AFM) in an aqueous electrolytic ambient [But92, Rai96, Hei99]. When the AFM

tip is in close proximity to the sample, the electrostatic force produced by their overlapping electrical double layers is detected by the AFM tip and correlated to charge density. This method is effective for measurements of biological samples in an aqueous environment. In non-aqueous environments, non-contact AFM methods have recently been used for the mapping of surface [Mor00] and interface [Lud01] charge on a semiconductor. However, these experiments require ultra high vacuum (UHV) and, in some cases, cooling of the system to liquid He temperature, which limit their application.

The Kelvin probe method, which can be applied at room temperature and pressure, uses a vibrating capacitor to measure the surface (or contact) potential difference between a sample and a vibrating electrode. The contact potential difference  $V_{CPD} = \Phi_{12} = \Phi_1 - \Phi_2 + \Phi_D$ , where  $\Phi_1$  and  $\Phi_2$  are work functions of the sample and the probe tip, respectively, and  $\Phi_D$  is the potential due to trapped charge that may exist on their surfaces. As the probe, which is biased at  $-V_b$  with respect to the sample, is dithered in close proximity to it, an AC current is induced by the modulation of the capacitance ( $C_K$ ) between them:  $i = (V_{CPD} + V_b)(dC_K/dt)$ . Theoretically,  $V_b$  is varied until the current goes to zero to determine  $V_{CPD}$ . In practice, the noise-limited rms current is monitored, and the bias which minimizes it is  $-V_{CPD}$ . This arrangement is illustrated for a semiconductor sample and metal probe in Fig. 1.

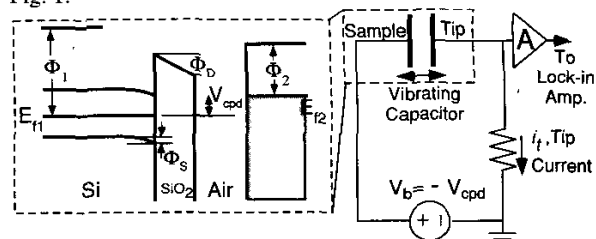


Fig. 1: (a-left) The energy band diagram for a sample with charged oxide on Si. (b-right) Simplified circuit diagram.

The reported device includes an actuator which provides the axial dither motion, the sense probe, which is electrically isolated from the actuator, and a lead transfer beam for the probe (Fig. 2). A wide isolation region is essential to minimize capacitive coupling between the drive signal of the actuator and probe. An insulating glass substrate also helps in this regard, as does the choice of actuator. The bent-beam actuator is electrothermally driven by passing current through the bent beam, which amplifies the resulting deformation into an outward motion of the tip

\* Contact information: EECS Dept., Univ. of Michigan, Ann Arbor, MI 48109-2122; tel: 734 615 6407; fax: 734 763 9324; email: yogesh@umich.edu

[Que01]. It is selected because it offers non-resonant dither motion with amplitude in the 10  $\mu\text{m}$  range with drive voltages of a few volts. The low voltage minimizes the coupling of the drive signal to the sense probe, while the large amplitude non-resonant displacement permits the dithering frequency and amplitude to be varied to suit the needs of the measurement. For measurements made along micromachined capillary channels, the electrical ground is provided by the conductive liquid present in the channel. However, the low conductivity of the liquid, and the long and narrow shape of the channel can make the access resistance to the point of measurement large, and create a slow RC time constant. To accommodate this, the dither frequency of the Kelvin probe is kept low, sacrificing sense current amplitude.

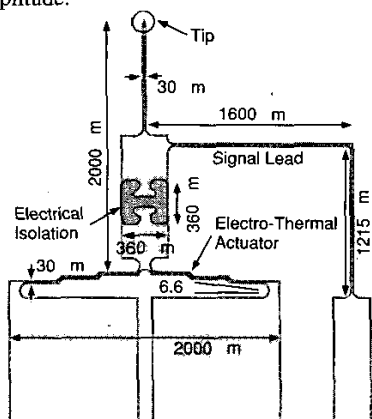


Fig. 2: Schematic of the  $\mu\text{EDM}$  Kelvin probe device showing the dimensions of the structure.

## II. FABRICATION

The micromachined Kelvin probe is fabricated by a modified micro electro-discharge machining ( $\mu\text{EDM}$ ) process. This technique is attractive because it can be used to fabricate parts from any electrically conductive material. Batch mode  $\mu\text{EDM}$ , performed with electroplated arrays of electrodes, offers very high throughput [Tak02]. However, normal  $\mu\text{EDM}$  by itself does not allow electrical isolation since all the mechanically connected features are also electrically connected. In the case of the micromachined Kelvin probe, the probe tip must be isolated from the dithering actuator, preferably by a large width of isolation to minimize the capacitive feed-through of the drive signal. This motivates the modified process that was developed.

The starting material is a commercially available 30  $\mu\text{m}$  thick stock metal sheet of MetGlas 2826MB; it is an alloy of primarily Ni and Fe (Fig. 3a). First, a traditional  $\mu\text{EDM}$  step is performed to define the shape of the epoxy plug in the work piece (Fig. 3b). The piece is removed from the  $\mu\text{EDM}$  oil bath and cleaned in an ultra-sonic bath with detergent. A quick-hardening two-part epoxy is properly mixed and applied onto the machined work piece to fill the plug (Fig. 3c). The epoxy is allowed to cure for over 12 hours to achieve proper mechanical stiffness and adhesion. A lapping step is performed for both sides of the work piece to

remove the excess cured epoxy (Fig. 3d). The work piece is cleaned before returning to the  $\mu\text{EDM}$  machine for the definition of the rest of the microstructure with the rest of the features aligned to the epoxy plug, which is released by cutting along its edges (Fig. 3e). Finally, the finished part is attached to a substrate for testing (Fig. 3f). A glass substrate is used to minimize parasitic capacitance that might cause the sensed signal to leak away. In a variant of the device, a larger Kelvin probe tip is attached onto the micromachined device for samples which may have coarse spatial variation or provide weak Kelvin probe signals. The larger tip has an area of 0.01  $\text{mm}^2$  and is made of tungsten. The finished structure is shown in Fig. 4.

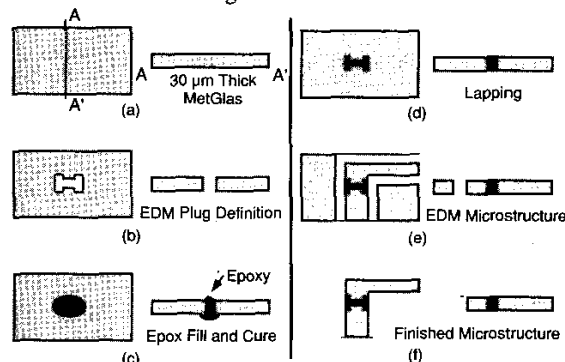


Fig. 3: The modified  $\mu\text{EDM}$  fabrication sequence to allow dielectric plugs and electrical isolation.

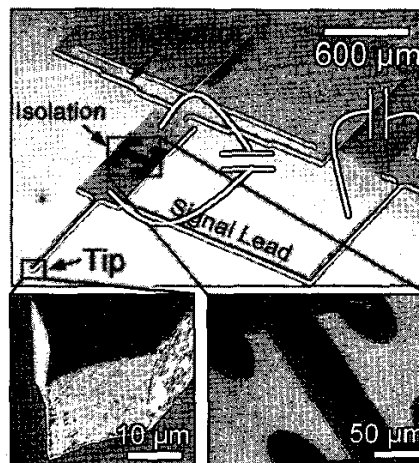


Fig. 4: SEM picture of the device and the close-up pictures of the tip area (lower left) and the isolation plug (lower right). The two parasitic capacitances shown are minimized.

## III. EXPERIMENTAL RESULTS

The operation of the integrated electro-thermal actuator is verified by supplying a current for actuation and monitoring the displacement of the tip using a calibrated optical method. The actuator generated a maximum displacement of 9  $\mu\text{m}$  when actuated at 85 mW with a resistance of 4.2  $\Omega$ . This satisfies the intended application.

The output of the Kelvin probe signal is a small time varying current signal related to the dither actuation. If a

parallel plate approximation is used for the capacitance between the probe and sample, the signal amplitude is:

$$i = (V_{CPD} + V_b) \cdot \frac{dC_K}{dt} = 2 \cdot f \cdot (V_{CPD} + V_b) \cdot \epsilon \cdot A \cdot \left( \frac{1}{g_0 - g_a} - \frac{1}{g_0} \right)$$

where  $f$  is the actuation frequency,  $\epsilon$  is the permittivity of the medium (air),  $A$  is the capacitor area,  $g_0$  is the initial capacitor gap, and  $g_a$  is the actuation displacement. Assuming an effective tip area of  $0.01 \text{ mm}^2$ ,  $V_{CPD} = 1 \text{ V}$ , actuation frequency of  $13 \text{ Hz}$ , and a capacitive gap of  $5 \text{ }\mu\text{m}$  (with 50% gap modulation due to actuation), the tip current is on the order of  $500 \text{ fA}$ . Hence, it is important to minimize noise from the measurement setup and electronics. The current signal is fed through a (SR 570) transconductance amplifier set at  $1 \text{ V/pA}$  and offering an input impedance of  $1 \text{ M}\Omega$  and then detected with a lock-in amplifier (SR 830 DSP) that is locked to the actuation frequency. The actuation frequency is carefully selected to avoid harmonics and sub-harmonics of common noise sources such as  $60 \text{ Hz}$  power line interference.

As the voltage bias between the probe and sample is varied to determine  $V_{CPD}$ , the observed rms current approaches a minimum value that is determined by the noise sources in the system (Fig. 5). The bias value that would eliminate the current in the absence of non-idealities must be extrapolated from tangents to the response curve drawn from high bias values, because at low currents the amplifier noise and parasitic feed-through from the drive signal can dominate even after carefully minimizing these effects. In our measurements, the rms noise floor is approximately  $150\text{--}200 \text{ fA}$ . When the nominal tip-to-sample separation is changed, the slope of current-to-bias response curve changes (Fig. 5). Artifacts from this are eliminated by keeping the tip-sample separation constant during a scan. Generally, this means that the slope of the rms tip current to  $V_b$  should be similar for all readings. These results were obtained with a tungsten tip of  $0.01 \text{ mm}^2$  sense area, and at  $13 \text{ Hz}$  dither.

The measurement setup for the microfluidic tests is shown in Fig. 6. Electrical access to the interior of the channel is provided through an Au electrode that is in contact with the fluid inside the channel but does not extend along its full length. The measured sense current for a pH 8 buffer is shown in Fig. 7. Both the magnitude and phase responses can provide the  $V_{CPD}$ . In the former, the lowest point is used to determine the contact potential, whereas in the phase plot, the point of maximum slope could be used.

Experiments were performed to determine relationship between the  $V_{CPD}$  above a single point of the micro-channel and the pH of the solution within it. The contact potentials for three different cases are plotted in Fig. 8, showing that the relationship is essentially linear. Acetic acid-sodium acetate and Tris-EDTA buffer systems are used to ensure that the pH in the channel is uniform and not affected by local residues when the system is flushed. A contact potential difference of  $\approx 6 \text{ V}$  is measured for a change in pH from 4 to 8 within the channel.

As indicated previously, the Kelvin probe can be used to map charge distribution over a sample surface area. This is useful in a number of contexts, particularly in assessing

plasma implantation and vacuum ultraviolet (VUV) photoemission. In order to evaluate the capability of the fabricated Kelvin probes in this regard, a test wafer was exposed to VUV radiation from a synchrotron to mimic charging due to photoemission during IC fabrication, as shown in Fig. 9a. Figure 9b shows the areal distribution of  $V_{CPD}$  on a charged sample that is obtained by exposing a Si wafer with  $359 \text{ nm}$  thick oxide to VUV radiation. Spatial variation of  $V_{CPD}$  from  $1\text{--}7 \text{ V}$  over a few hundred microns is evident. The position of the peak corresponds to the center of the VUV exposure.

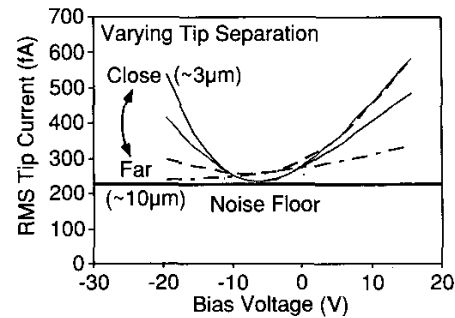


Fig. 5: The Kelvin probe signal obtained at different gap separation; this result indicates that when the tip is too far, the signal is not reliable.

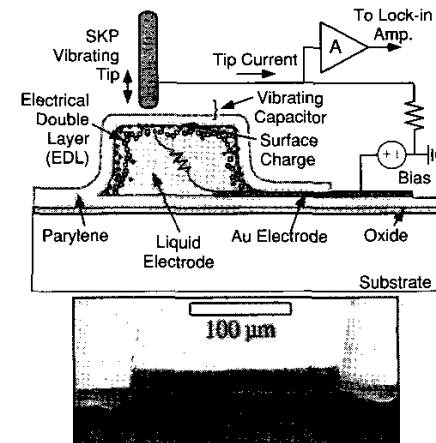


Fig. 6: (a-upper) Measurement of pH using Kelvin probe. (b-lower) The microfluidic channel used in the measurements had  $3\text{--}5 \text{ }\mu\text{m}$  thick parylene walls and was  $20 \mu\text{m}$  high [Man97].

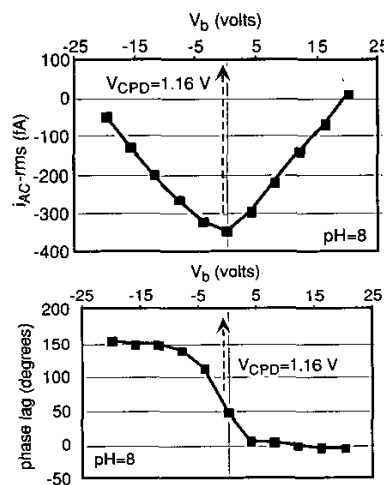


Fig. 7: Measured sense current amplitude and phase at a single spot above the micro-channel with a tip-sample spacing of  $\approx 5 \mu\text{m}$  and dither amplitude of  $\approx 2 \mu\text{m}$ . Both plots contain offset values which are inconsequential.

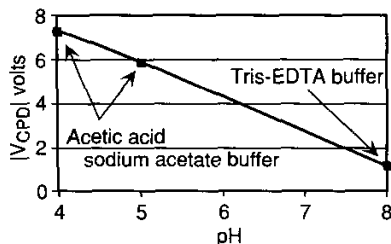


Fig. 8: Measured  $V_{CPD}$  showing linear dependence on pH, which was calibrated using a pH meter (Piccolo, Hanna Instruments) of 0.01 pH resolution and accuracy.

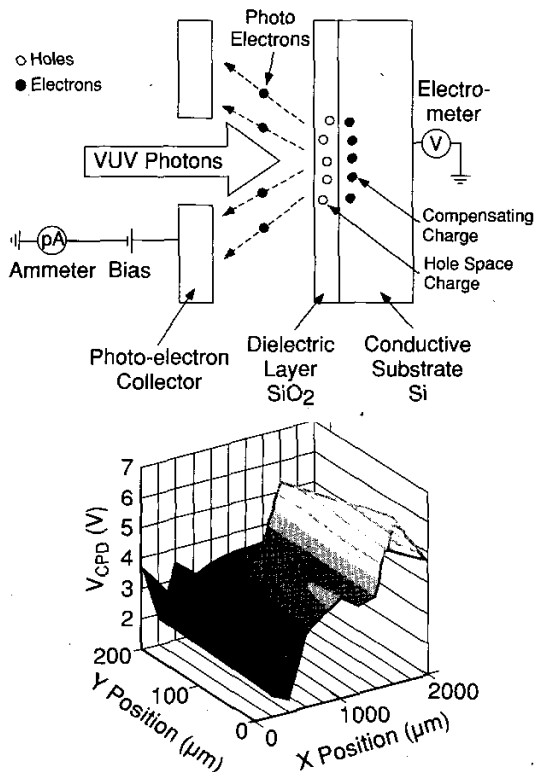


Fig. 9: (a) Charging during IC fabrication emulated by exposing a Si wafer with 359 nm thick oxide to vacuum UV synchrotron radiation. (b) Areal map of the resulting  $V_{CPD}$  showing a portion of the exposed region.

#### IV. CONCLUSIONS

A micromachined Kelvin probe device with integrated dither actuator is presented in this work. The electrothermal actuator achieves a maximum of 9  $\mu\text{m}$  displacement when actuated at 85 mW. The Kelvin probe tip is electrically isolated from the actuator using a modified  $\mu\text{EDM}$  process that permits wide expanses dielectric materials to be embedded in the structure. The device is successfully used to measure the 2D charge variation in  $\text{SiO}_2$  on a Si substrate and solution variations of pH in a microfluidic channel. This effort demonstrates that a relatively simple micro-structure and can be used to provide surface potential measurements

in a non-invasive manner, and that these are useful in both semiconductor and microfluidic diagnostics. In the latter context, it is possible to envision microfluidic system with a Kelvin probe integrated above critical positions in the channel, permitting integrated in-line measurements in real time to control chemical reactions.

#### Acknowledgements

The authors are grateful to Prof. F. Terry of UM and Mr. Jason Lauer of UW for helpful discussions. Mr. Lauer also performed the synchrotron exposures. This effort was supported in part by an National Science Foundation Career award to YG, and performed in part at the University of Wisconsin Synchrotron Radiation Center which is supported in part by the National Science Foundation under grant number DMR-0084402.

#### REFERENCES

- [And52] J.R. Anderson, A.E. Alexander, "Theory of the vibrating condenser converter and application to contact potential measurements," *Australian Journal of Applied Science*, 3, 201, 1952
- [But92] H.-J. Butt, "Measuring local surface charge densities in electrolyte solutions with a scanning force microscope," *Biophysical Journal*, 63(2), pp. 578-582, 1992
- [Cis98] C. Cismaru, J.L. Shohet, K. Nauka, J.B. Friedmann, "Relationship between the charging damage of test structures and the deposited charge on unpatterned wafers exposed to an electron cyclotron resonance plasma," *Appl. Phys. Lett.*, 72(10), p. 1143-5, 1998
- [Fan92] S. Fang, J.P. McVittie, "Thin-oxide damage from gate charging during plasma processing," *IEEE Electron Dev. Lett.*, 13, p. 288, 1992
- [Fri97] J.B. Friedmann, J.L. Shohet, R. Mau, N. Hershkovitz, S. Bisgaard, S. Ma, J.P. McVittie, "Plasma-parameter dependency of thin-oxide damage from wafer charging during electron-cyclotron-resonance plasma processing," *IEEE Trans. Semic. Mfg.*, 10(1), 154, '97
- [Hei99] W.F. Heinz, J.H. Hoh, "Relative surface charge density mapping with the atomic force microscope," *Biophysical J.*, 76, pp. 528-38, '99
- [Hof97] A. Hoff, K. Nauka, T. Persson, J. Lagowski, L. Jastrzebski, P. Edelman, "A novel approach to monitoring of plasma processing equipment & plasma damage without test structures," *IEEE/SEMI Advanced Semic. Manufacturing Conf.*, 185, 1997
- [Lud01] R. Ludeke, E. Cartier, "Imaging of oxide and interface charges in  $\text{SiO}_2\text{-Si}$ ," *Microelectronic Engineering*, 59, pp. 259-263, 2001
- [Man97] F. Man, D.K. Jones, C.H. Mastrangelo, "Microfluidic plastic capillaries on silicon substrates: a new inexpensive technology for bioanalysis chips," *IEEE MEMS, Nagoya, Japan*, pp. 311-6, 1997
- [Mor00] S. Morita, M. Abe, K. Yokoyama, Y. Sugawara, "Defects & their charge imaging on semiconductor surfaces by non-contact atomic force microscopy & spectroscopy," *J. Crystal Grth*, 210, p. 408-15, '00
- [Mur73] P.V. Murphy and S. Merchant, "Blood Compatibility of polymer electrets", *Proc. Int. Conf. On Electrets, Charge Storage, and Transport in Dielectrics*, Miami Beach, FL, Electrochemical Society, Princeton, NJ, pp. 627-649, 1973
- [Nab97] W. Nabhan, B. Equer, "A high-resolution scanning Kelvin probe microscope for contact potential measurements on the 100 nm scale," *Review of Scientific Instruments*, 68(8), pp. 3108, 1997
- [Que01] L. Que, J.S. Park, Y.B. Gianchandani, "Bent-beam electrothermal actuators-I: single beam & cascaded devices," *J. Microelectromech. Sys.*, 10(2), pp. 247-254, 2001
- [Rai96] R. Raiteri, M. Grattarola, H.-J. Butt, "Measuring electrostatic double-layer forces at high surface potentials with the atomic force microscope," *Journal of Physical Chemistry*, 100, pp. 16700-5, 1996
- [Sur70] N.A. Surplice, R.J.D'Arcy, "A critique of the Kelvin method of measuring work functions," *J. Physics E: Scientific Instrum* 3, 477, 1970.
- [Tak02] K. Takahata, Y.B. Gianchandani, "Batch mode micro-electrodischarge machining," *J. Microelectromech. Sys.*, 11(2), p. 102-10, '02